



OPEN ACCESS

EDITED BY

Denny Oliveira,
University of Maryland, Baltimore County,
United States

REVIEWED BY

Alexei V. Dmitriev,
Lomonosov Moscow State University, Russia
Vladimir A. Sreckovic,
University of Belgrade, Serbia

*CORRESPONDENCE

Kai Schennetten,
✉ kai.schennetten@dlr.de

RECEIVED 19 September 2024

ACCEPTED 04 November 2024

PUBLISHED 25 November 2024

CITATION

Schennetten K, Matthiä D, Meier MM, Berger T
and Wirtz M (2024) The impact of the Gannon
Storm of May 2024 on the radiation fields at
aviation altitudes and in low earth orbits.
Front. Astron. Space Sci. 11:1498910.
doi: 10.3389/fspas.2024.1498910

COPYRIGHT

© 2024 Schennetten, Matthiä, Meier, Berger
and Wirtz. This is an open-access article
distributed under the terms of the [Creative
Commons Attribution License \(CC BY\)](#). The
use, distribution or reproduction in other
forums is permitted, provided the original
author(s) and the copyright owner(s) are
credited and that the original publication in
this journal is cited, in accordance with
accepted academic practice. No use,
distribution or reproduction is permitted
which does not comply with these terms.

The impact of the Gannon Storm of May 2024 on the radiation fields at aviation altitudes and in low earth orbits

Kai Schennetten*, Daniel Matthiä, Matthias M. Meier,
Thomas Berger and Michael Wirtz

German Aerospace Center, Institute of Aerospace Medicine, Radiation Biology, Cologne, Germany

In May 2024 the strongest geomagnetic storm since the Halloween storms of 2003 occurred. Media reported worldwide about the space weather situation and its effects on the infrastructure. Of particular interest were reports claiming severe effects on the radiation exposure at aviation altitudes, although no data supporting this assertion were available at that time. In this work the different aspects that affect the radiation exposure at aviation altitudes are discussed for the event. Furthermore, the corresponding dose rates are evaluated and compared to data from Low Earth Orbit. Model calculations indicate an additional contribution to the radiation field at aviation altitudes due to this extraordinary space weather situation, although the dose rates were still in the lowest category D0 of the space weather D-index, i.e., within the dose rate variation of a solar cycle.

KEYWORDS

space weather, solar energetic particle (SEP), ground level enhancement (GLE), radiation field, low earth orbit (LEO), radiation protection, aviation

1 Introduction

Polar lights are a fascinating natural phenomenon. On rare occasions, they can even be observed at mid-latitudes, e.g., in Central Europe, during strong geomagnetic storms. A series of such events occurred between 10 and 13 May 2024, which peaked on 11 May classified as G5 storm on the NOAA G-scale (Poppe and Jorden, 2006) and referred to as Gannon Storm, e.g., in the International Space Weather Action Teams (ISWAT) community (Tobiska, 2024; Lugaz et al., 2024). It was the strongest geomagnetic storm since the Halloween storms of 2003. The events were associated with several solar flares and coronal mass ejections from Active Region 13664 which emerged entirely on the visible side of the Sun on 1 May 2024 and grew in size to its maximum extent of 14 Earth areas on 10 May 2024 (SWPC, 2024a). Media reported worldwide about the space weather situation and raised awareness of the potential adverse effects on technology. For example, strong geomagnetic storms cause Geomagnetically Induced Currents (GICs), the potential effects of which include damage in long conductors, e.g., power transmission lines, railway infrastructure or oil pipelines (Gannon, 2019; Thaduri et al., 2020).

Furthermore, potential effects of this geomagnetic storm on the radiation field at aviation altitudes have also been reported on by the international press. Of particular

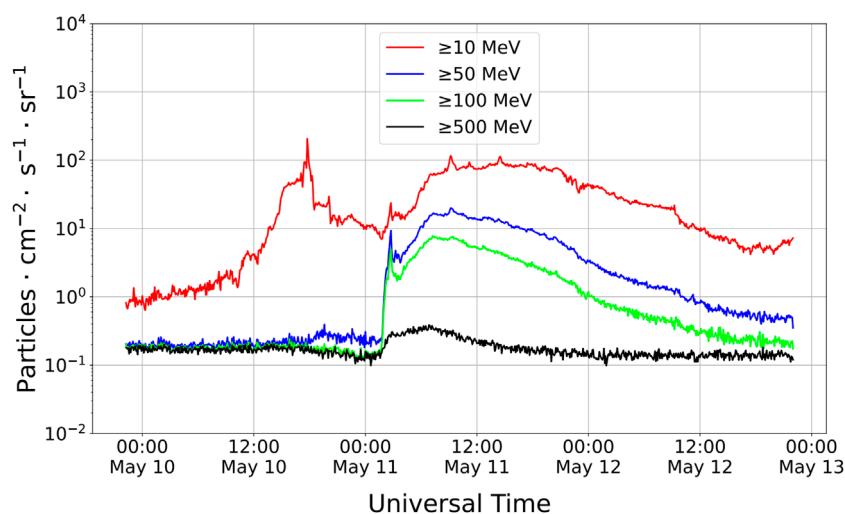


FIGURE 1
Temporal evolution of the integral proton flux during the event.

interest has obviously been a sensational representation of the Gannon space weather event. For example, an article by Jonathan O'Callaghan and Lee Billings published in *Scientific American* insinuated that the Gannon Storm even had a severe impact on the radiation exposure of aircrews and passengers. Stakeholders were unsettled by statements such as “Flight trackers showed airlines rerouting planes to avoid Earth's poles, where crews and passengers would have been exposed to worrisome spikes in cosmic radiation from the storm” (O'Callaghan and Billings, 2024), although no scientific evidence for this statement was given in the article. However, since visible aurorae and the mentioned adverse effects on technology are the result of strongly increased fluxes of solar particles, it is important to investigate how these particles might actually have affected the radiation fields in the near-Earth space environment and even at aviation altitudes. Although the Earth is generally effectively shielded from cosmic radiation by its magnetic field and its atmosphere, radiation levels at aviation altitudes are increased with regard to the Earth's surface due to the omnipresent galactic cosmic radiation. Since the corresponding job-related radiation exposure of aircrew is in the range of the legally regulated exposures of terrestrial radiation workers, aircrew have been included in the statutory radiation protection regulations in many countries, e.g., in the European Union for many years (EU, 1996; EU, 2013). A fundamental radiation protection principle requires aircraft operators to keep the radiation exposure due to cosmic radiation as low as reasonably achievable. Although corresponding protection measures are hardly possible for the galactic cosmic radiation component, effective measures are feasible during rare solar radiation events, e.g., reducing the flight altitude with or without adapting the Mach number (Matthiä et al., 2015).

A prerequisite for an increase in the radiation intensity at aviation altitudes is an increase in the flux of solar particles with energies above about 500 MeV. This information is nowadays available from the website of the Space Weather Prediction Center (SWPC) of the National Oceanic and Atmospheric Administration (NOAA) (SWPC, 2024b). However, the traditional S-scale alert for

solar radiation storms is based on the increase in the total number of the impinging particles above 10 MeV, about 99% of which do generally not contribute to the radiation field at aviation altitude because of their spectral energy distribution and the atmospheric shielding. Therefore, the space weather D-index has been introduced for this particular radiation field. The D-index is based on the additional dose rate due to solar energetic particles at aviation altitudes instead of the flux of incoming particles at the location of the GOES satellite in a geosynchronous orbit outside the Earth's atmosphere (Meier and Matthiä, 2014). The first alert phase D1 is triggered when the additional dose rate exceeds $5 \mu\text{Sv/h}$. An analysis of previous solar energetic particle events by Kataoka et al. has demonstrated that a D1-alert is hardly possible without a concomitant Ground Level Enhancement (GLE), which is the result of corresponding increases in the count rates of at least two neutron monitors measured on ground (Kataoka et al., 2015). On 10 May 2024 at 13:35 UTC, SWPC issued an S-scale solar radiation storm alert which peaked at 17:45 UTC as an S2-alert on the same day with a maximum flux of particles above 10 MeV of 207 pfu (SWPC, 2024c) and caused an immediate and distinct Forbush decrease, a reduction in cosmic ray intensity caused by the suppression of galactic cosmic rays by a CME and the embedded magnetic field. An increase in the flux of particles with energies above 500 MeV was observed aboard the GOES satellite on the following day at about 02:00 UTC finally resulting in a small Ground Level Enhancement, which was counted as GLE 74. Since a GLE, even a very small one, is indicative of a potential alert on the D-scale, a corresponding analysis based on available data is required to meet the demands for information of the stakeholders, e.g., in the aviation industry.

2 Methods

Since comprehensive measurements at aviation altitudes during the event were not available, model calculations using the Professional Aviation DOse CALculator (PANDOCA) were

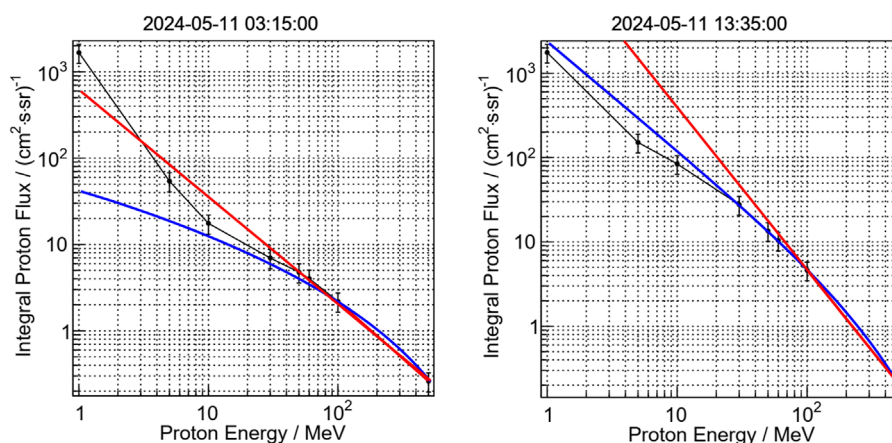


FIGURE 2
Integral proton spectra (GOES18) at the beginning of the event (left) and a few hours later (right) with the corresponding fits with the Band function (blue) and the power law function (red).

performed to quantify the different effects on the radiation dose at aviation altitudes during the event. For this purpose, the total effective dose for a hypothetical flight from FRA to LAX with a duration of 10:22 h was calculated for different scenarios. For simplicity the flight route is approximated as great circle and the altitude is set to a constant flight level of the upper commercial airspace (FL380, FL400, FL430) to create the worst-case in terms of dose impact. This is a more tangible approach from an operational perspective compared to just calculating dose rates at fixed points in the atmosphere. The various contributing effects that can both increase and decrease the dose rates at aviation altitudes are discussed separately (Section 3.1). Additionally, the radiation environment in Low Earth Orbit (LEO) is assessed by providing direct dose measurements taken aboard the Eu:CROPIS satellite conducted with the RAMIS radiation detector at approximately 600 km. A comparison of the radiation dose at aviation altitudes and the measurements in LEO will demonstrate how effective the shielding capability of the atmosphere really is (Section 3.2).

2.1 PANDOCA

The PANDOCA model (Matthiä et al., 2014; Meier et al., 2018) was developed at the German Aerospace Center (DLR) for the assessment of the exposure in aviation from cosmic radiation. It is based on transport calculations of primary protons and alpha particles through the atmosphere using the PLANETOCOSMICS application (Desorgher et al., 2006) to the Geant4 Monte-Carlo framework (Agostinelli et al., 2003; Allison et al., 2006; Allison et al., 2016). Applying different types of conversion coefficients to the calculated particle fluence rate at a given altitude, a number of dose quantities can be calculated, e.g., ambient dose equivalent, effective dose (ICRP, 2007), absorbed dose in water or silicon, etc. PANDOCA contains an implementation of the galactic cosmic radiation (GCR) model by Matthiä et al. using a single parameter to account for the variations of the galactic cosmic ray intensity during the solar cycle (Matthiä et al., 2013). Additionally, it can be used with arbitrary primary proton spectra. A number of strong solar energetic

particle events were analyzed with the PANDOCA model in the past (Matthiä, 2009; Matthiä et al., 2009; Matthiä et al., 2015).

To account for the shielding from the magnetic field of the Earth, the model includes a pre-calculated map of cut-off rigidities for quiet geomagnetic conditions but alternative sets for the cut-off rigidity can be employed for geomagnetically disturbed periods. The default map of cut-off rigidities used by PANDOCA was calculated with PLANETOCOSMICS for the 10th generation of the International Geomagnetic Reference Field (IGRF) (Maus et al., 2005). For geomagnetically disturbed periods, the IGRF is coupled with an external field model by Tsyganenko (1989), which can be set to different states corresponding to different levels of geomagnetic disturbance, the strongest corresponding to $K_p \geq 6-$.

In this work, the PANDOCA model was used to estimate the different effects of the event on the dose rate at aviation altitudes: the Forbush decrease caused by the suppression of the primary galactic cosmic ray intensity, the variation of the geomagnetic shielding effect and the impact of the solar energetic particles (SEP).

Variations of the galactic cosmic ray intensity were derived from Oulu neutron monitor count rates (Section 2.1.1). The impact of the geomagnetic storm on the cut-off rigidities and the exposure was estimated based on the maximum value of K_p during the event. The increase in dose rates in the atmosphere was calculated using different fits on the GOES integral proton data (Section 2.1.2).

2.1.1 NM Oulu

The model for the GCR intensity used in PANDOCA has a single parameter W (Matthiä et al., 2013). This parameter can be derived from measurements, for instance neutron monitor count rates. Matthiä et al. (2013) provided a linear relationship between W and Oulu Neutron Monitor count rates. In this work pre-event and in-event neutron monitor count rates are used to estimate the impact of the event on the effective dose at flight altitude from GCR.

Neutron monitor count rates can also be used to estimate the energy spectrum of large solar energetic particle events (Matthiä, 2009; Matthiä et al., 2009; Matthiä et al., 2015; Copeland et al., 2008) by evaluating the response of Neutron Monitors at

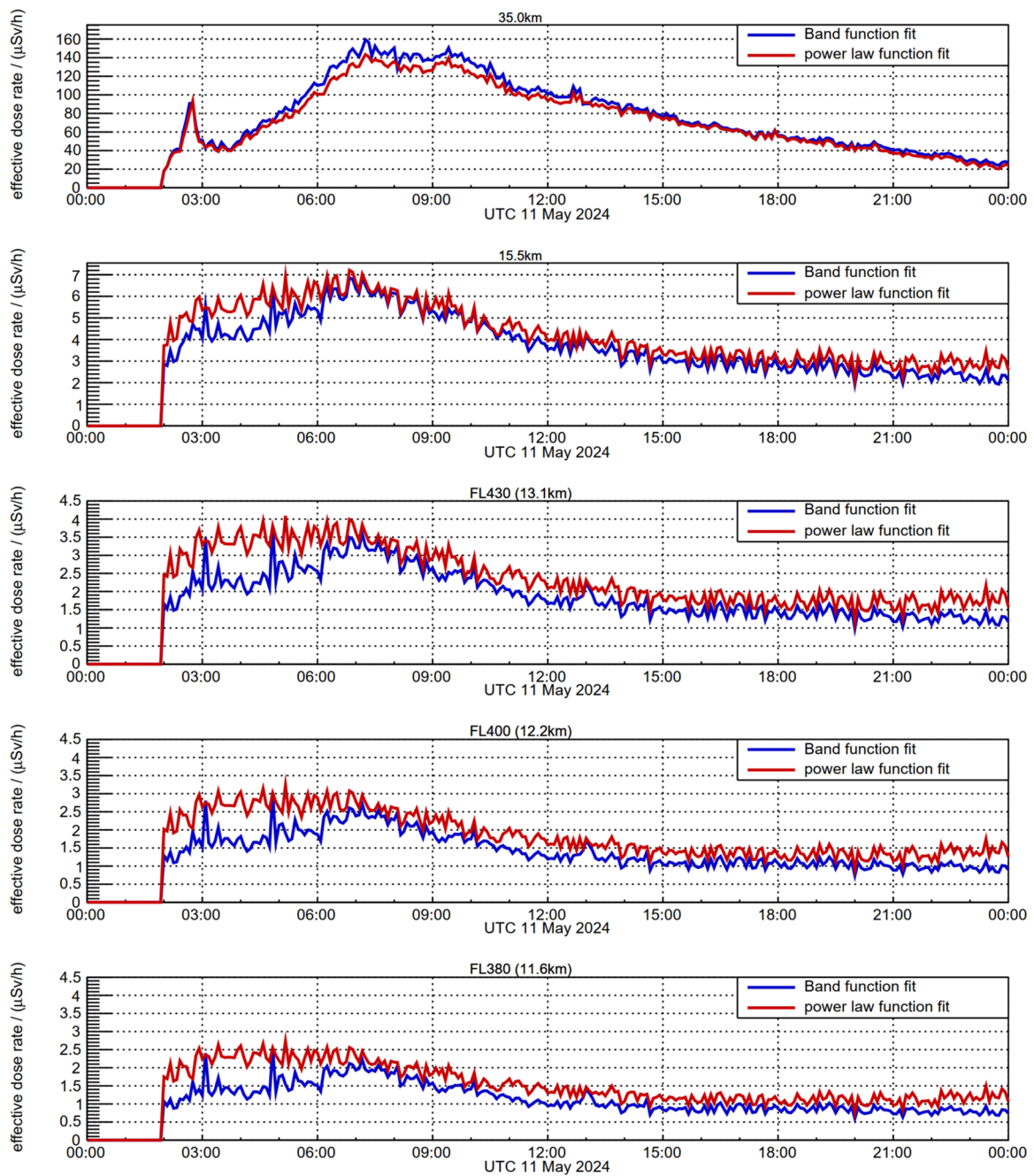


FIGURE 3 Effective dose rates calculated for different altitudes with PANDOCA during the event at locations without magnetic shielding ($R_c = 0$ GV).

TABLE 1 Worst case estimate of total additional effective dose due to solar energetic particles for a flight from FRA to LAX. The results for both functions used for the fitting of the GOES proton spectra are listed.

	Total effective dose due to SEP		
	FL430	FL400	FL380
Band function fit	25 µSv	19 µSv	15 µSv
Power law fit	32 µSv	25 µSv	21 µSv

locations of different geomagnetic shielding. The event in May 2024, however, was not strong enough to apply this technique. Therefore, the model calculations were based solely on measurements of the Geostationary Operational Environmental Satellites (GOES).

2.1.2 Spectral fits of GOES proton data

In order to estimate the dose rates at aviation altitudes during the event, the GOES integral proton spectra (Figure 1) were fitted with

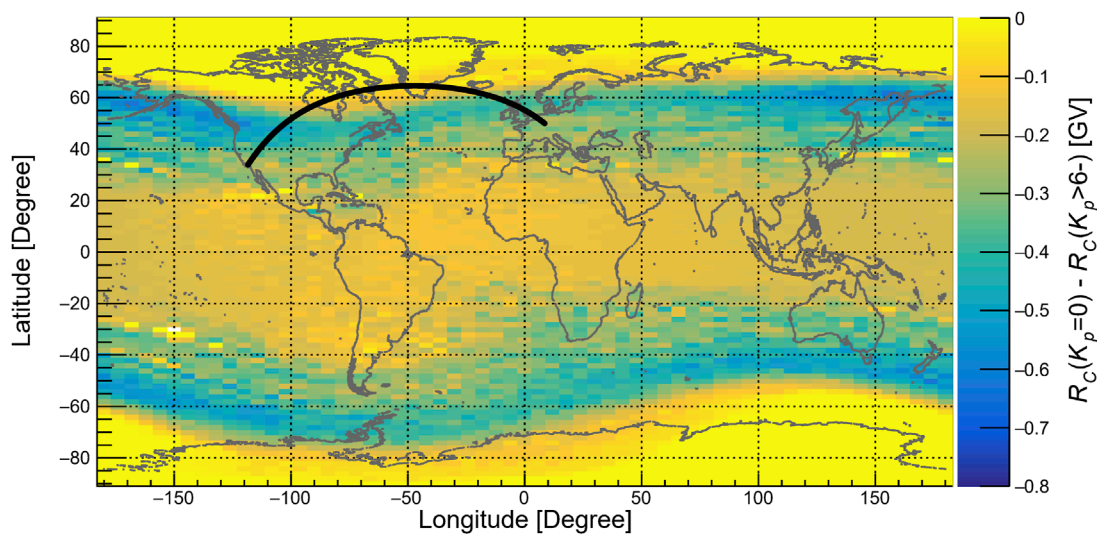


FIGURE 4 Map of the difference in cut-off rigidity for $K_p = 0$ and $K_p > 6$. The calculated difference in cut-off rigidity is most pronounced in mid-latitudes. The black line shows the flight from FRA to LAX used for dose calculations.

TABLE 2 Total effective dose due to GCR calculated for different flight levels for a flight from FRA to LAX with and without a shift of cut-off rigidities due to geomagnetic disturbances.

	FL430	FL400	FL380
Total effective dose (undisturbed)	63.0 μSv	55.5 μSv	50.3 μSv
Total effective dose (disturbed)	63.4 μSv	55.8 μSv	50.6 μSv
Relative difference	+0.6%	+0.5%	+0.6%
Absolute difference	+0.4 μSv	+0.3 μSv	+0.3 μSv

two different functions: a simple power law in energy and a double power law with exponential transition [band function (Band et al., 1993)] that is often used to fit energetic particle spectra. Five-minute averaged integral proton fluxes were used as provided by SWPC for the primary GOES (GOES-18 at the time).

In order to avoid fitting the quiet time background, a trigger for proton fluxes above 100 MeV was set to 0.5 pfu, i.e., $f(E > 100 \text{ MeV}) > 0.5 \text{ cm}^{-2} \text{ s}^{-1} \text{ sr}^{-1}$. When this threshold is exceeded, the integral proton spectrum is fitted with the Band function in the energy range between 20 MeV and 500 MeV and with the power law spectrum between 100 MeV and 500 MeV. The rationale behind the different energy ranges is to get a better understanding of the impact of the different energies. As the energy spectrum tends to bend at lower energies, the fit of the Band spectrum is usually more accurate in this range. However, with decreasing altitudes, higher energies become more and more important and an extrapolation of the spectrum to energies above 500 MeV, which is the highest data point in the integral proton measurements, is necessary. At 41,000 ft, for instance, the vertical shielding of the air corresponds to approximately 180 g/cm^2 , i.e., a proton needs an energy of at least 600 MeV to reach that deep into the atmosphere.

Two examples for the results of the fit during the event are illustrated in Figure 2: at the beginning of the event (03:15 UTC) and more than 10 hours into the event (13:35 UTC). While the proton flux at lower energy continued to increase during this time, the flux above 500 MeV decreased, which is also visible in Figure 1. This led to a steeper spectrum at later times. It is also obvious that the constraint of the Band function at lower energies also leads to a steeper spectrum compared to the single power law. It can, of course, not be excluded that the spectrum at energies above 500 MeV falls even more rapidly, but we hypothesize that the extrapolation of the Band function serves as a lower estimate for the real spectrum while the single power law serves as an upper estimate.

2.2 RAMIS detector

RAMIS is a silicon detector telescope developed at DLR and currently flying on the DLR Eu:CROPIS satellite mission at approximately 600 km altitude polar orbit (Hauslage et al., 2018; Guo et al., 2023). The telescope consists of two circular Passivated Implanted Planar Silicon detectors FD50-14-300RM (Canberra) with a thickness of 300 μm and an area of 0.817 cm^2 . The detectors are separated by 7.3 mm which leads to an opening angle of the telescope of 109°. RAMIS provides the count- and dose rates in 1-min cadence for the top detector and energy deposition spectra for both diodes in a 5-min cadence. Based on the energy deposition spectra measured in coincidence in both detectors the linear energy transfer (LET) spectra are deduced. The energy deposition range in Si ranges from 0.09–145 MeV thereby also covering a LET range in H_2O from 0.15–228 $\text{keV}/\mu\text{m}$. RAMIS is mounted on the satellite and the top detector is covered by 3 mm aluminum, i.e., for vertical incidence, sensitive to protons with energies above 24.3 MeV and electrons above 1.38 MeV.

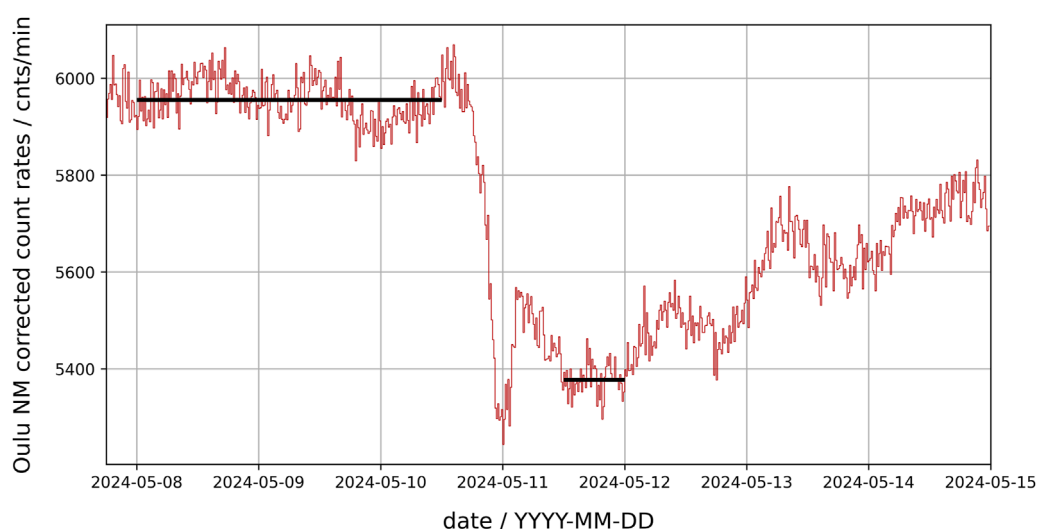


FIGURE 5

Pressure corrected count rate of the Oulu neutron monitor during the Forbush Event. The black horizontal lines indicate the mean count rates for the assumed two scenarios (5955.3 counts/min before Forbush decrease and 5378 counts/min during Forbush decrease).

TABLE 3 Total effective dose due to GCR calculated for different flight levels for a flight from FRA to LAX with and without Forbush effect.

	FL430	FL400	FL380
Pre-event	66.4 μ Sv	58.5 μ Sv	53.0 μ Sv
Forbush event	50.7 μ Sv	45.0 μ Sv	41.1 μ Sv
Relative difference	-23.6%	-23.1%	-22.5%
Absolute difference	-15.7 μ Sv	-13.5 μ Sv	-11.9 μ Sv

3 Results and discussion

3.1 Dose at aviation altitudes

During such a series of events there are mainly three different effects that may influence the radiation exposure at aviation altitudes. First of all, there is the SEP component which can provide an additional dose to the GCR component of the field. This requires solar protons with sufficient energies to contribute. The second effect is a shift of cut-off rigidities which can lead to an increased GCR component due to weaker geomagnetic shielding in mid-latitudes caused by the geomagnetic storm. The third effect arises from an additional shielding of the GCR indicated by the ongoing pronounced Forbush decrease, when the GLE event occurred. This means the dose rates due to GCR were already lower compared to levels without an event. Thus, in total there are two effects that can increase and one effect that decreases the radiation exposure during the event. These effects are assessed individually and compared with each other to quantify their significance for the radiation exposure at aviation altitudes.

The hypothetical flight route used for these dose calculations covers mid-latitudes where the shift in cut-off rigidity takes place, in specific high latitudes (max. 64.6°N), and altitudes (FL430) where the impact of the SEPs is most pronounced. The dose results for all three effects are then compared to calculations for the same flight under undisturbed space weather conditions, i.e., without any event.

3.1.1 Increase of effective dose rates during the SEP event

The integral proton spectra from the fit to the GOES data (section 2.1.2) were converted to differential spectra in the energy range from 10 MeV to 10 GeV and applied to the PANDOCA model for different altitudes and a cut-off rigidity of 0 GV for a worst-case estimation without geomagnetic shielding. The resulting effective dose rates during the event are illustrated in Figure 3. The calculated effective dose rates started to rise at 01:55 UTC on 11 May 2024 and the calculated peak dose rates were reached between 04:00 UTC and 07:00 UTC. For FL430, FL400, and FL380 increases in the effective dose rate of approximately 4 μ Sv/h, 3 μ Sv/h, and 2.5 μ Sv/h were estimated, which lasted for about 6 h. Within the next 6 h, the additional dose rate decreased to about 1.5 μ Sv/h. Rated by the space weather D-index these dose rates are still in the lowest category of D0, i.e., within the variation of a solar cycle and no cause for concern or further action. Above commercial aviation altitudes the D-index reached D1 at 15.5 km. At an even higher altitude of 35 km it reached D5. It should be noted that the model calculations do not account for additional shielding by the aircraft or other masses, which can be neglected at higher atmospheric shielding. In particular, the atmospheric shielding at aviation altitudes (>190 g/cm²) is much greater than the shielding effects of the skin of the fuselage (<0.5g/cm²) (Copeland, 2017). The effects of other masses in the aircraft are also quite low, which is why such shielding effects can usually be neglected for aircraft dosimetry (Battistoni et al., 2005).

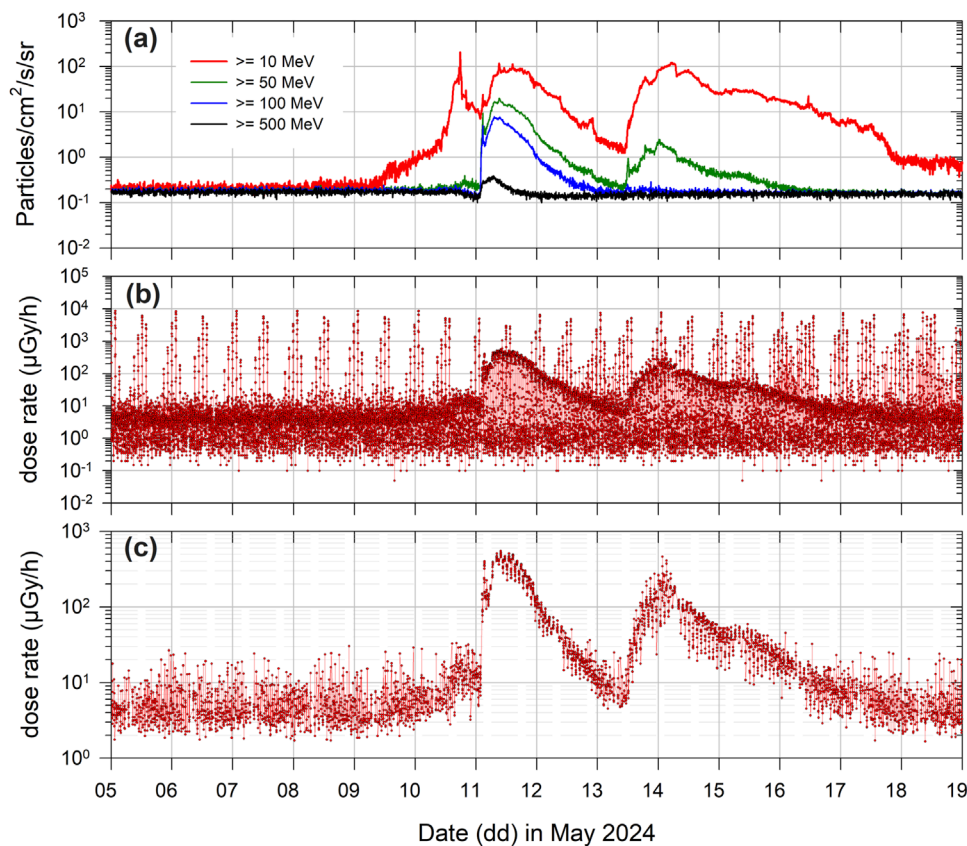


FIGURE 6
5 May to 19 May 2024. (A) GOES proton flux, (B) RAMIS dose rate ($\mu\text{Gy/h}$), (C) RAMIS dose rate after the cut on geomagnetic latitude.

At 35 km, however, any additional shielding may be relevant and the dose rates are to be understood as estimates for the exposure free in air.

For a conservative estimation of the additional dose due to this SEP event, a cut-off rigidity of 0 GV was assumed for the whole model flight. It was also assumed that the whole flight path with a duration of 10:22 h was impacted by the event. Under these conditions the total effective dose due to SEPs was 25 μSv –32 μSv for the model flight at FL430, 19 μSv –25 μSv at FL400, and 15 μSv –21 μSv at FL380. The results for the total additional effective dose are shown in Table 1 for both functions used for fitting the proton spectra.

3.1.2 Impact of magnetic shielding variation

The considered flight path from FRA to LAX leads directly through mid-latitude regions where the effect of a cut-off rigidity shift due to geomagnetic disturbances is most pronounced (Figure 4). The reference flight is calculated for the K_p index 0 and a W-parameter of 99.58, which corresponds to the monthly mean in May 2024. The calculated difference in the total effective dose of the flights during undisturbed and disturbed geomagnetic conditions is only on the order of 0.6% or 0.4 μSv (Table 2) for FL430, which is negligible compared to other influences that affect the dose.

3.1.3 Reduction in effective dose during the forbush decrease

Approximately 8 hours prior to the GLE a pronounced Forbush event set in (Figure 5), which resulted in a decreased count rate of the Oulu neutron monitor of up to 10% with regard to the baseline before the event. When the GLE started, the count rate increased by some 4%. The total effective doses of the reference flight were compared for undisturbed conditions and during the minimum of the Forbush decrease. The 60-h mean count rate before the onset of the Forbush event is used for the calculation of the reference flight. For the calculation of the total flight dose during the Forbush event the mean count rate for a period of 12 h after the GLE had decreased is determined. These two mean count rates (black horizontal lines in Figure 5) are converted into their corresponding W-parameters for the two compared flights, i.e., 84.9 and 138.5.

The results for the total effective dose of the flights for different flight levels are shown in Table 3. The decrease in dose for all listed altitudes is about 23%, e.g., the reduction in dose is about 15.7 μSv at FL430.

3.2 SEPs in low earth orbit

The atmosphere provides excellent shielding against cosmic radiation. For GLE 74, this is demonstrated by a comparison of

RAMIS measurements in LEO with the calculated dose rates at aviation altitudes. Figure 6A shows the GOES integral proton flux for different energy ranges for 5–19 May 2024. In Figure 6B the dose rate in silicon measured with the RAMIS top detector for the same time span is depicted. This graph shows the complete dose rate data including passages through the inner radiation belt (South Atlantic Anomaly) and the outer radiation belt. The graph in Figure 6C illustrates the effects of the SEPs with data restricted to high geomagnetic latitudes. While the average absorbed dose rate in Si was $(5.3 \pm 3.4) \mu\text{Gy/h}$ before the event (1–9 May 24), a maximum dose rate of $548 \mu\text{Gy/h}$ was reached on 11 May 09:48 UTC. Applying a Silicon-to- H_2O conversion factor of 1.23 and a quality factor of 1.29 results in a maximum dose equivalent rate of $870 \mu\text{Sv/h}$ which corresponds to D8 on the D-scale. In terms of dose rate by SEPs this is more than two orders of magnitude higher compared to aviation altitudes.

3.3 Discussion

The various effects on the radiation exposure at aviation altitudes were calculated separately using PANDOCA. For this, a model flight (FRA-LAX) impacted by all these different effects was used for the calculation of total flight dose for different altitudes. The contribution to the total flight dose due to the shift in cut-off rigidity is negligible with an additional dose of only 0.5% or $0.3 \mu\text{Sv}$ – $0.4 \mu\text{Sv}$. If the dose reduction of the Forbush decrease is subtracted from the dose increase caused by solar particles, the total increase is in the range of $9 \mu\text{Sv}$ – $16 \mu\text{Sv}$ on a flight from Frankfurt to Los Angeles for FL430, which is an extra 14%–24% of the total effective dose compared to a flight without any event. However, it should be noted that the sequence of events does not necessarily have to be the same in every case. Not every G5 event is associated with solar particles with a corresponding fraction of sufficiently high energy protons which are required to contribute to the radiation field at aviation altitudes. Nor does a GLE always happen in the middle of a Forbush event that reduces the additional dose. Without the Forbush decrease and the concomitant lowered dose rates compared to pre-event conditions (–23%), the theoretical additional dose due to SEP to the total flight dose would have been in the range of 38%–48%. This is no cause for concern, as the corresponding dose rates from solar particles at aviation altitudes up to 13 km are still rated as only D0 ($<5 \mu\text{Sv/h}$). A slight increase to the D1 alert level can be assessed for an altitude of 15.5 km. However, the radiation exposure at an altitude of 35 km might have already reached D5 level with a further increase to D8 in Low Earth Orbits (LEOs), e.g., in the orbit of the Eu:CROPIS satellite at 600 km.

4 Conclusions

The Gannon Storm of May 2024 is a further example of a space weather situation with a small GLE that did not even trigger the first (pre-)alert phase on the D-scale for the radiation field of civil aviation at 13 km altitude, i.e., the temporary increase in radiation was within the natural variation during a solar cycle (cf. Matthiä et al., 2018; Tobiska et al., 2018; Copeland et al.,

2018). In LEOs, i.e., outside the Earth's atmosphere, however, the situation was completely different and the additional radiation exposure due to the Gannon Storm might have even triggered a D8 alert. This demonstrates the high shielding capacity of the Earth's atmosphere against solar radiation. The impinging solar particles have to traverse the magnetosphere of the Earth and penetrate correspondingly deep into its atmosphere to contribute to the radiation exposure at cruising altitudes, which strongly depends on their energy distribution. Therefore, each solar particle event has to be analyzed individually in order to assess a potential additional exposure inside the Earth's atmosphere.

The news coverage of this event seemed to be focused on the fact that this event was the first in over 20 years which reached the highest level on the NOAA G-Scale. Although this event actually made a small contribution to the radiation field at aviation altitudes, the media and public should not infer that a strong event on the G-scales gives an indication of the actual radiation exposure at aviation altitudes.

Summary of main conclusions:

- SEPs during the Gannon Storm contributed to the radiation field at aviation altitudes, which does not necessarily have to be the case for every G5 event.
- Dose rates due to SEPs were low at aviation altitudes (D0, i.e., $<5 \mu\text{Sv/h}$)
- Dose rates at LEOs reached up to D8 ($870 \mu\text{Sv/h}$)
- All effects combined result in 14%–24% of additional total effective dose for a flight from Frankfurt to Los Angeles at FL430.

Data availability statement

The raw data supporting the conclusions of this article will be made available by the authors, without undue reservation.

Author contributions

KS: Writing–original draft, Writing–review and editing. DM: Writing–original draft, Writing–review and editing. MM: Writing–original draft, Writing–review and editing. TB: Writing–original draft, Writing–review and editing. MW: Writing–original draft.

Funding

The author(s) declare that financial support was received for the research, authorship, and/or publication of this article. This work was partly funded within the framework of the DLR project “Resiliente Technologien für den Katastrophenschutz” (RESITEK) that aims to pool DLR's capabilities and technologies in the fields of aeronautics, space, energy, transport, and security in order to strengthen effective and resilient disaster prevention and crisis management.

Acknowledgments

We would like to thank the Sodankylä Geophysical Observatory and the website team (<http://cosmicrays oulu.fi>) for providing the Oulu neutron monitor data. We acknowledge the SWPC subscription service for providing space weather information.

Conflict of interest

The authors declare that the research was conducted in the absence of any commercial or financial relationships

References

- Agostinelli, S., Allison, J., Amako, K., Apostolakis, J., Araujo, H., Arce, P., et al. (2003). GEANT4-a simulation toolkit. *Nucl. Instrum. and Methods Phys. Res. Sect. a-Accelerators Spectrom. Detect. Assoc. Equip.* 506, 250–303. doi:10.1016/s0168-9002(03)01368-8
- Allison, J., Amako, K., Apostolakis, J., Araujo, H., Dubois, P. A., Asai, M., et al. (2006). Geant4 developments and applications. *IEEE Trans. Nucl. Sci.* 53, 270–278. doi:10.1109/tns.2006.869826
- Allison, J., Amako, K., Apostolakis, J., Arce, P., Asai, M., Aso, T., et al. (2016). Recent developments in GEANT4. *Nucl. Instrum. and Methods Phys. Res. Sect. a-Accelerators Spectrom. Detect. Assoc. Equip.* 835, 186–225. doi:10.1016/j.nima.2016.06.125
- Band, D., Matteson, J., Ford, L., Schaefer, B., Palmer, D., Teegarden, B., et al. (1993). BATSE observations of gamma-ray burst spectra. I-Spectral diversity. *Astrophysical J.* 413, 281–292. doi:10.1086/172995
- Battistoni, G., Ferrari, A., Pelliccioni, M., and Villari, R. (2005). Evaluation of the doses to aircrew members taking into consideration the aircraft structures. *Space Life Sci. Aircr. Space Radiat. Environ.* 36, 1645–1652. doi:10.1016/j.asr.2005.04.037
- Copeland, K., Sauer, H. H., Duke, F. E., and Friedberg, W. (2008). Cosmic radiation exposure of aircraft occupants on simulated high-latitude flights during solar proton events from 1 January 1986 through 1 January 2008. *Adv. Space Res.* 42, 1008–1029. doi:10.1016/j.asr.2008.03.001
- Copeland, K., Matthiä, D., and Meier, M. (2018). Solar cosmic ray dose rate assessments during GLE 72 using MIRA and PANDOCA. *Space weather* 16, 969–976. doi:10.1029/2018sw001917
- Copeland, K. (2017). *Approximating shielding effects on galactic cosmic radiation effective dose rate calculations during extreme altitude and sub-orbital flights using CARI-7/7A*. Oklahoma: FAA Civil Aerospace Medical Institute.
- Desorgher, L., Flückiger, E. O., and Gurtner, M. (2006). The PLANETOCOSMICS Geant4 application. *36th COSPAR Sci. Assem.* 36, 2361.
- EU (1996). *Council Directive 96/29/Euratom of 13 May 1996 laying down basic safety standards for the protection of the health of workers and the general public against the dangers arising from ionizing radiation*. Luxembourg: Official Journal of the European Union.
- EU (2013). *Council Directive 2013/59/EURATOM of 5 December 2013 laying down basic safety standards for protection against the dangers arising from exposure to ionising radiation, and repealing Directives 89/618/Euratom, 90/641/Euratom, 96/29/Euratom, 97/43/Euratom and 2003/122*. Luxembourg: Official Journal of the European Union.
- Gannon, J. (2019). The infrastructure impacts of solar storms. *Eos* 100. doi:10.1029/2019eo135665
- Guo, J., Li, X., Zhang, J., Dobynde, M. I., Wang, Y., Xu, Z., et al. (2023). The first ground level enhancement seen on three planetary surfaces: Earth, moon, and mars. *Geophys. Res. Lett.* 50. doi:10.1029/2023gl103069
- Hauslage, J., Strauch, S. M., Eßmann, O., Haag, F. W. M., Richter, P., Krüger, J., et al. (2018). Eu:CRISP – “euglena gracilis: combined regenerative organic-food production in space” - a space experiment testing biological life support systems under lunar and martian gravity. *Microgravity Sci. Technol.* 30, 933–942. doi:10.1007/s12217-018-9654-1
- ICRP (2007). The 2007 recommendations of the international commission on radiological protection. ICRP publication 103. *Ann. ICRP* 37, 1–332. doi:10.1016/j.icrp.2007.10.003
- Kataoka, R., Nakagawa, Y., and Sato, T. (2015). Radiation dose of aircrews during a solar proton event without ground-level enhancement. *Ann. Geophys.* 33, 75–78. doi:10.5194/angeo-33-75-2015
- Lugaz, N., Knipp, D., Morley, S. K., Liu, H., Hapgood, M., Carter, B., et al. (2024). Memoriam of editor jennifer L. Gannon. *Space Weat.* 22 (6). doi:10.1029/2024SW004016
- Matthiä, D., Heber, B., Reitz, G., Sihver, L., Berger, T., and Meier, M. (2009). The ground level event 70 on december 13th, 2006 and related effective doses at aviation altitudes. *Radiat. Prot. Dosim.* 136, 304–310. doi:10.1093/rpd/ncp141
- Matthiä, D., Berger, T., Mrigakshi, A. I., and Reitz, G. (2013). A ready-to-use galactic cosmic ray model. *Adv. Space Res.* 51, 329–338. doi:10.1016/j.asr.2012.09.022
- Matthiä, D., Meier, M. M., and Reitz, G. (2014). Numerical calculation of the radiation exposure from galactic cosmic rays at aviation altitudes with the PANDOCA core model. *Space weather* 12, 161–171. doi:10.1002/2013sw001022
- Matthiä, D., Schaefer, M., and Meier, M. M. (2015). Economic impact and effectiveness of radiation protection measures in aviation during a ground level enhancement. *J. Space Weather Space Clim.* 5, A17. doi:10.1051/swsc/2015014
- Matthiä, D., Meier, M. M., and Berger, T. (2018). The solar particle event on 10–13 september 2017: spectral reconstruction and calculation of the radiation exposure in aviation and space. *Space weather* 16, 977–986. doi:10.1029/2018SW001921
- Matthiä, D. (2009). *The radiation environment in the lower atmosphere: a numerical approach*. Diss: Christian-Albrechts-Universität.
- Maus, S., Macmillan, S., Chernova, T., Choi, S., Dater, D., Golovkov, V., et al. (2005). The 10th-generation international geomagnetic reference field. *Geophys. J. Int.* 161, 561–565. doi:10.1111/j.1365-246x.2005.02641.x
- Meier, M. M., and Matthiä, D. (2014). A space weather index for the radiation field at aviation altitudes. *J. Space Weather Space Clim.* 4, A13. doi:10.1051/swsc/2014010
- Meier, M. M., Copeland, K., Matthiä, D., Mertens, C. J., and Schennetten, K. (2018). First steps toward the verification of models for the assessment of the radiation exposure at aviation altitudes during quiet space weather conditions. *Space weather* 16, 1269–1276. doi:10.1029/2018sw001984
- Muhlestein, B., and SWPC(2024a). The Evolution and Impact of active region 13664 – an operational perspective. *Nat. oceanic and atmos. admini*. Available at: <https://storymaps.arcgis.com/stories/0c501560633549b69dbd01c4c725b2b3>
- O’Callaghan, J., and Billings, L. (2024). *The strongest solar storm in 20 Years did little damage, but worse space weather is coming*. New York, NY. Available at: <https://www.scientificamerican.com/article/the-strongest-solar-storm-in-20-years-did-little-damage-but-worse-space/>.
- Poppe, B., and Jorden, K. (2006). *Sentinels of the Sun*. Boulder. Johnson Books.
- SWPC (2024b). 500 MeV proton flux now. Available at: <https://www.swpc.noaa.gov/news/goes-500-mev-proton-flux-observations-now-available> (Accessed August, 09 2024).
- SWPC (2024c). Product subscription service SUMMARY: proton event 10 MeV integral flux exceeded 10 pfu (S1). *Space Weather Message Code*. SUMPX1, Serial Number: 111.
- Thaduri, A., Galar, D., and Kumar, U. (2020). Space weather climate impacts on railway infrastructure. *Int. J. Syst. Assur. Eng. Manag.* 11, 267–281. doi:10.1007/s13198-020-01003-9
- Tobiska, W. K., Meier, M. M., Matthiä, D., and Copeland, K. (2018). Characterizing the variation in atmospheric radiation at aviation altitudes. *Extreme Events Geosp.* 453–471. doi:10.1016/b978-0-12-812700-1.00018-2
- Tobiska, W. K. 2024. RE: personal communication.
- Tsyganenko, N. (1989). A magnetospheric magnetic field model with a warped tail current sheet. *Planet. Space Sci.* 37, 5–20. doi:10.1016/0032-0633(89)90066-4

that could be construed as a potential conflict of interest.

Publisher’s note

All claims expressed in this article are solely those of the authors and do not necessarily represent those of their affiliated organizations, or those of the publisher, the editors and the reviewers. Any product that may be evaluated in this article, or claim that may be made by its manufacturer, is not guaranteed or endorsed by the publisher.